A Journal of the Gesellschaft Deutscher Chemiker
Angewandte
GDCh
International Edition
Chemie
www.angewandte.org

# Accepted Article

**Title:** A Two-photon H2O2-activated CO Photoreleaser

**Authors:** Yong Li, Yingzheng Shu, Muwen Liang, Xilei Xie, Xiaoyun Jiao, Xu Wang, and Bo Tang



**To be cited as:** *Angew. Chem. Int. Ed.* 10.1002/anie.201805806
*Angew. Chem.* 10.1002/ange.201805806

**Link to VoR:** http://dx.doi.org/10.1002/anie.201805806
http://dx.doi.org/10.1002/ange.201805806

WILEY-VCH

10.1002/anie.201805806


WILEY-VCH

# A Two-photon $H_2O_2$-activated CO Photoreleaser

Yong Li, Yingzheng Shu, Muwen Liang, Xilei Xie, Xiaoyun Jiao, Xu Wang* and Bo Tang*

**Abstract:** Carbon monoxide (CO) is proposed as an active pharmaceutical agent with promising pharmic prospect, as it has been involved in multifaceted modulation of diverse physiological and pathological processes. However, questions remain for therapeutic application of inhaled CO attributed to the inherent great affinity between CO and hemoglobin. Therefore, a robust platform with function of CO-carrying and controllable releasing, depending on the local status of organism, is of prominent significance for effectively avoiding the side effects of CO-inhaling and optimizing the biological regulation function of CO. Herein, utilizing oxidative stress biomarker $H_2O_2$ as a trigger and combining with photo control technique, we present a two-photon $H_2O_2$-activated CO photoreleaser, **FB**, featuring capacity of highly sensitive and specific $H_2O_2$ sensing and meanwhile, photocontrollable CO releasing. By capitalizing on the outstanding features of **FB**, the $H_2O_2$ sensing and CO photo-releasing were successfully implemented and visualized *in vitro* and *in vivo*. With the aid of **FB**, the evidence of oxidative stress associated with $H_2O_2$ upon angiotensin II administration was provided, and the directly visual proof of vasodilation effect of CO was obtained. Therefore, we anticipate that the superior features of **FB** will endow it with potential application for oxidative stress warning and oxidative stress-mediated CO controlled release.

Carbon monoxide (CO), generated endogenously by enzymatic heme metabolism in mammals, has widely emerged as crucial physiological gasotransmitter featuring cytoprotective effect and maintaining cellular homeostasis, thus endowing it with potential drug activity. As such, the efficient delivery of CO in the organism has received much attention.[1] Unfortunately, attributed to the inherent great affinity between CO and hemoglobin, multiple uncontrollable issues emerge in direct CO gas inhalation, such as dose control, targeted delivery, etc. This often leads to a high level of carboxyhemoglobin and results in CO poisoning, making it difficult to implement CO's physiological and medical effects.[2] Therefore, it is of urgent need to develop CO carrier aiming at sustained or controlled CO releasing. Currently, two types of molecules have been employed as CO releasers, transition metal carbonyl complexes and small organic molecules.[3] Compared with the potential cytotoxicity caused by heavy metal, the organic molecular CO releasers with improved biocompatibility have attracted increasing attention, especially those triggered in controllable fashions.[4] Recently, organic photo-triggered CO releasers have demonstrated appealing profile as it promises precise spatiotemporal control.[5]

In general, normal level of reactive oxygen species (ROS) is critical for the regulation of diverse physiological processes. However, the outburst of excessive amounts of ROS, namely oxidative stress, can induce cell damages, ultimately leading to various human diseases.[6] Up to date, CO has emerged as a promising therapeutic agent against various disease modes in associated with oxidative stress [1,7] Thus, ROS may act as a potential intracellular trigger for precise CO-releasing. Hydrogen peroxide ($H_2O_2$) is regarded as a typical factor responsible for cellular oxidative damage as it is one of the key contributors in the redox signaling modulation.[8] Consequently, the fluctuation of $H_2O_2$ may become a modulator for controllable CO releasing. However, the photo-release of CO are manipulated by extracellular irradiation only, which fails to be triggered by the intracellular oxidative stress status.[5] As is known to all, fluorescence combined with confocal microscope, especially two-photon imaging technology, demonstrates unique capacity of visualizing dynamical biological events with high-contrast spatiotemporal resolution and less phototoxicity.[9] Therefore, utilizing fluorescent imaging to trace CO-releasing process and map its physiological effects is of prominent significance for deeply understanding the biological benefits of CO.

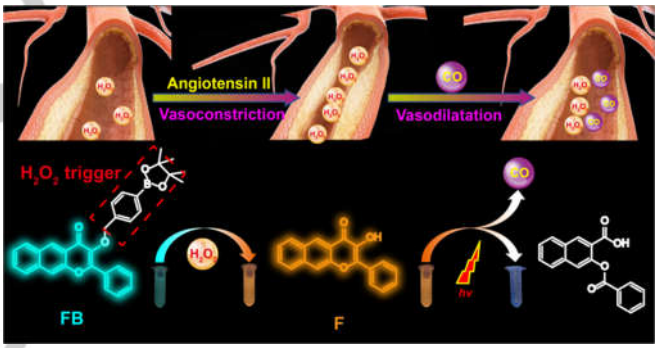


**Scheme 1.** The chemical structure of **FB** and the corresponding proposed CO photo-releasing mechanism.

Hence, in this work, we engineered a flavonol-borate-conjugate, **FB**, for precise CO-releasing with guiding of $H_2O_2$, a biomarker of intracellular oxidative stress. **FB** was firstly employed as a fluorescent sensor for $H_2O_2$ via "off-on" behavior of excited state intramolecular proton transfer (ESIPT) triggered by borate deprotection.[10] After tracing of $H_2O_2$, the activated flavonol (**F**) was subsequently irradiated to release CO (Scheme 1).[5c] Therefore, we reasoned that **FB** could function for both $H_2O_2$ tracing and $H_2O_2$-guided CO releasing.

The detailed synthetic procedures are shown in Scheme S1. With **FB** in hand, its spectral property was firstly evaluated. As expected, **FB** itself exhibited maximal absorbance/emission at 375 nm (ε = 12000 $L \cdot mol^{-1} \cdot cm^{-1}$)/485 nm (Figure S1). By sharp contrast, in the presence of $H_2O_2$, the solution underwent a bathochromic shift in the maximal absorption wavelength (405 nm) and presented two fluorescence emission peaks at 480 nm and 585 nm, respectively, in which the later emission band with larger stokes shift can be attributed to the recovery of ESIPT effect due to the liberation of protected hydroxyl group in **F**. The photostability of **FB** and **F** (with xenon lamp of fluorophotometer, 360 W, slit width: 2 nm/2 nm) were assessed to confirm no

[*] Y. Li, Y. Shu, M. Liang, Dr. X. Xie, Dr. X. Jiao, Pro. X. Wang, Pro. B. Tang
College of Chemistry, Chemical Engineering and Materials Science, Key Laboratory of Molecular and Nano Probes, Ministry of Education, Collaborative Innovation Center of Functionalized Probes for Chemical Imaging in Universities of Shandong, Institute of Molecular and Nano Science, Shandong Normal University, Jinan 250014, P. R. China. E-mail: tangb@sdnu.edu.cn, wangxu@sdnu.edu.cn

Supporting information for this article is given via a link at the end of the document.

photolysis occurred during spectral scanning (Figure S2). Subsequently, the ratiometric response of **FB** towards $H_2O_2$ was investigated (Ratio= $I_{585\ nm}/I_{485\ nm}$). Gratifyingly, as showed in Figure 1, **FB** displayed a gradual increasing in ratio value in the presence of different concentrations of $H_2O_2$, and manifested an approximately 19-fold ratiometric enhancement upon 5 equivalents of $H_2O_2$ addition. The ratio intensity of **FB** possessed an outstanding linear relationship ($R^2$ = 0.998) with $H_2O_2$ concentration with a regression equation of *Ratio* = 0.39062 + 0.1451 [$H_2O_2$] (μM). The limit of detection was calculated as low as 66 nM. In addition, the dependence of absorption intensity upon reaction time was evaluated. Upon the addition of 10 equivalents of $H_2O_2$, the signal displayed a drastic increment within 13 min, then leveled off, indicating the high reactivity of **FB** towards $H_2O_2$ (Figure S3).

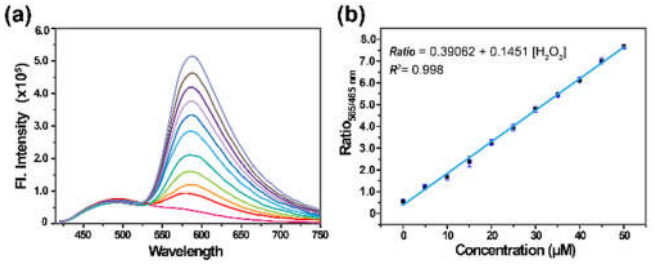


**Figure 1.** The $H_2O_2$ detection capability of **FB**. (a) Fluorescent response of 10 μM **FB** to $H_2O_2$ (0−50 μM) in PBS buffer solution (50 mM, pH 7.4) with 10% $CH_3CN$. (b) The linear curve of ratio (585/485 nm) derived from fluorescent titration.

Next, the specificity of **FB** was investigated and the results displayed that no obvious ratio change of **FB** was triggered after exposed to various active species which commonly exist in biological systems, thus implying the high specificity of **FB** towards $H_2O_2$ (Figure S4). In addition, the influence of pH was also carried out to confirm that **FB** can be potentially applied to trace $H_2O_2$ in physiological environment (Figure S5). The proposed mechanism for detecting $H_2O_2$ was verified with high resolution mass spectra (HRMS) and the result was found a mass peak at m/z 289.0873 (Figure S6), which was in good agreement with **F** as displayed in Scheme 1.

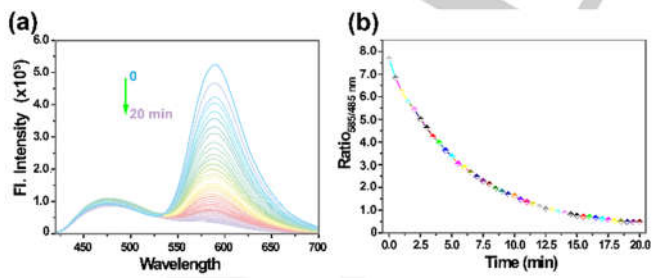


**Figure 2.** The $H_2O_2$-dependent CO-releasing of **FB**. Fluorescent intensity changes of $H_2O_2$-loaded **FB** (10 μM) solution during irradiation (λ= 405 nm, CEL-HXF300 Xenon lamp with power 15 mW/cm$^2$). (a) and the corresponding ratio variation (b).

The capacity of the $H_2O_2$-activated CO-releasing capability of **FB** was performed during light irradiation (λ= 405 nm, CEL-HXF300 Xenon lamp with power 15 mW/cm$^2$). In the absence of $H_2O_2$, satisfactory photostability of **FB** itself was observed through the constant fluorescent intensity during irradiation (Figure S7). In the presence of $H_2O_2$, gradually decreasing fluorescent signals at 585 nm were detected upon the increase of irradiation time (Figure 2). On the contrary, no obvious ratio variation of FB solution was detected when it was kept in the dark upon $H_2O_2$ activation (Figure S8). In view of the photolysis products emiting no fluorescent signal when excited with 405 nm, these results suggested the effective occurence of the photo-induced CO-releasing. Meanwhile, as can be seen from Figure 2b, the fluorescent ratio readout sharply attenuated within first few minutes, indicating a quick CO release during irradiation and low phototoxcity in living system (Figure S9). These results suggested that **FB** can be employed as a potent $H_2O_2$-dependent one-photon-induced CO releaser.

Then, the proposed photolysis mechanism for CO-releasing process was validated. It was reported in previous work that two compounds were formed in this photolysis reaction. One of photolysis products, CO, was certified utilizing CO fluorescent probe **ACP-2**, which reported by our lab previously (Figure S10).[7] As shown in Figure S11, fluorescence enhancement of **ACP-2** after irradiation consolidated the releasing of CO. After that, the solution was analyzed by HRMS. A discriminable mass signal at m/z 291.0665 (M-H) was presented (Figure S12), which corresponding to another photolysis product, 3-(benzoyloxy)-2-naphthoic acid. Collectively, both fluorescent analysis and HRMS detection provided an evidence for the proposed mechanism of photodecomposition as displayed in Scheme 1, which also displayed good consistency with the previous work.[5c]

With data manifesting that **FB** can serve a bifunctional platform for $H_2O_2$ detection and CO photoreleasing, the imaging capability of **FB** was demonstrated. Firstly, the MTT assay was performed to check the biocompatibility and the results indicated that these compounds exhibited low cytotoxicity, as the experimental concentration in cells was far less than the $IC_{50}$ value (Figure S13). Subsequently, the potential TP excited capacity was explored. Encouragingly, Both **FB** and **F** displayed high TP absorption cross-section (δ) at 800 nm as 30 GM (1 GM = $10^{-50}$ cm$^4$ s photon$^{-1}$) and 96 GM, respectively, implying these two compounds can be effectively excited by TP laser. And the liver tissue depth imaging assays manifested that **FB** displayed a discriminable fluorescent signal at depth up to 153 μm upon TP excitation (Figure S14). Furthermore, a mass spectra signal of photolysis product, 3-(benzoyloxy)-2-naphthoic acid, was also obtained when $H_2O_2$-loaded **FB** solution was exposed to TP irradiation (Figure S15), thus implying that two-photon can also effectively induce photolysis of **F**. Similar to the preceding verification with one-photon irradiation, the CO-releasing profile of **FB** was confirmed in vascular smooth muscle cells (VSMCs) with TP laser irradiation using **ACP-2** (Figure S16). Collectively, **FB** can be served as a robust TP fluorescent imaging tool as well as a $H_2O_2$-activated TP-induced CO releaser.

Afterwards, the $H_2O_2$ tracing ability of **FB** was verified in live cells. Upon phorbol myristate acetate (PMA, a well-defined $H_2O_2$ intracellular inducer) treatment, an obvious ratio increment was obtained (Figure S17), which can be efficiently attenuated by N-acetyl-L-cysteine (NAC, a well-validated $H_2O_2$ scavenger). In addition, this fluorescent ratio increment exhibited no discriminable attenuation when the cells were pretreated with L-NAME ($N^G$-Nitro-L-arginine Methyl Ester Hydrochloride, which can suppress peroxynitrite up-regulation through Inhibiting nitric oxide synthase activity). These results suggested that the ratio enhancement was indeed resulted from up-regulation of $H_2O_2$

concentration. Then, the PMA dose-dependent $H_2O_2$ fluctuation was explored. Prior to cells imaging, VSMCs were pretreated with NAC to eliminate the intracellular basal $H_2O_2$. Subsequently, the cells were exposed to various doses of PMA. As can be seen from Figure 3 (a-e), fluorescence signal in VSMCs displayed a significant and PMA dose-dependent ratiometric change. The data demonstrated that **FB** was a powerful tool to map $H_2O_2$ fluctuation in live cells.

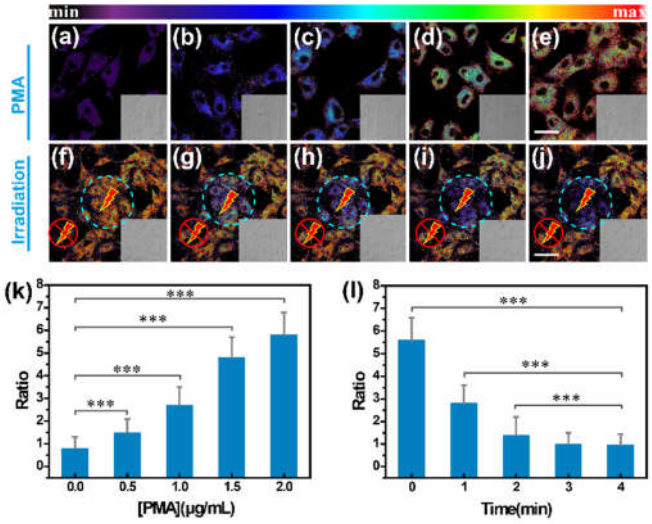


**Figure 3.** The $H_2O_2$ mapping and CO releasing in vitro**.** (a−e) The NAC (1.0 mM, 1 h) pretreated VSMCs were incubated various concentrations of PMA (0, 0.5, 1.0, 1.5, 2.0 μg/mL) for 3 h and then exposed to **FB** (20 μM, 15 min). (f−j) The VSMCs were coincubated with PMA (2.0 μg/mL, 3 h), followed by stained with **FB**, and then the cells inside the selected circle were irradiated with two-photon laser at 800 nm for different time (0, 1, 2, 3, 4 min). (k) The ratio changes of cells in (a−e). (l) The ratio changes of cells in the circle of (f−j). Ratio=$F_{420–510\ nm}/F_{520–620\ nm}$. The values are the mean ± s.d. for n = 3, **p < 0.01, ***p <0.001. Scale bar = 25 μm (a-e) and 50 μm (f-j).

Subsequently, the CO-release ability was investigated in live cells utilizing TP. The VSMCs were co-incubated with PMA followed by stained with **FB**, and then the cells were imaged during light irradiation. As shown in Figure 3 (f-j), the cells in given circle were irradiated with TP laser while the other outside were not. It can be observed that only the cells in the given circle displayed a remarkable ratiometric signal attenuation whereas the adjacent unstimulated area presented no obvious variation. In addition, the VSMCs in the given circle displayed a gradually attenuated ratio signal upon the increase of irradiation time. Taken together, the results indicated that $H_2O_2$-activated CO-releasing process can be effectively induced and monitored by TP laser in precise spatiotemporal controllable fashion.

Having well-established the $H_2O_2$ detection ability and the succedent TP-induced CO-releasing *in vitro*, the *in vivo* assays were carried out in larval zebrafish. Firstly, the $H_2O_2$ tracing was performed. After NAC pretreatment, the increased ratio caused by PMA administraion was efficiently suppressed, demonstrating **FB** was capable of mapping $H_2O_2$ fluctuation in zebrafish (Figure S18). Then, time-dependent ratiometric readout upon PMA administration was captured. As can be seen from Figure 4 (a-f), the time-dependent ratiometric signal increment was obtained, demonstrating the increased $H_2O_2$ level. Afterward, the TP-induced CO release was investigated. As shown in Figure 4 (g-l), temporal and spatial ratio value changes in the region of interest (ROI) during irradiation indicated precisely spatio-temporal controllable CO release. Taken together, it is credible to draw the conclusion that **FB** can be applied as a potent platform for real-time $H_2O_2$ monitoring and $H_2O_2$-activated TP-induced CO release *in vivo*.

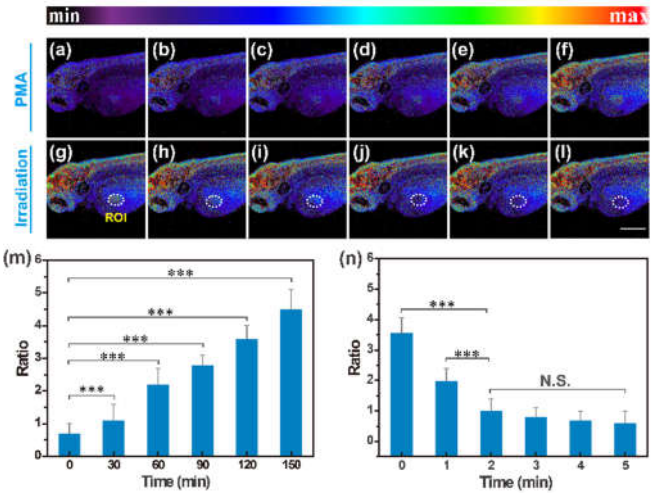


**Figure 4.** The $H_2O_2$ mapping and CO-releasing in vivo. (a-f) The zebrafish was pretreated with NAC (1.0 mM, 1 h), and then loaded with **FB** (20 μM, 15 min), followed by administrated with PMA (2.0 μg/mL). (g-l) The region of interest (ROI) of the zebrafish (f) was irradiated with 800 nm laser. (m) The ratio changes of (a-f). (n) The ratio changes of ROI in (g-l). Ratio=$F_{420–510\ nm}/F_{520–620\ nm}$. The values are the mean ± s.d. for n = 3, ***p <0.001. N.S. denoted no significant. Scare bar = 250 μm.

It was reported that angiotensin II, a potent peptide hormone vasoconstrictor for hypotension and hypovolemia treatment, can induce deleterious effects on mitochondria through overproduction of $O_2^{\bullet-}$.[11] However, as one of the key contributors in modulation of intracellular redox signaling, $H_2O_2$ fluctuation in angiotensin-II-induced physiological events is much less clear. Meanwhile, CO is a well-known promoter for vasorelaxation through several signal pathways.[12] Nonetheless, to the best of our knowledge, no straightforward and visualized evidence of vasodilating capability of CO was demonstrated. Therefore, encouraged by the excellent behavior of **FB** *in vitro* and *in vivo*, an attempt was made to simultaneously address the above two issues by using **FB**. Firstly, oxidative stress associated with $H_2O_2$ upon angiotensin II treatment and the CO vasorelaxation effect were evaluated *in vitro*. Cyclic guanosine monophosphate (cGMP), a vasodilative biomarker generated through the activation of soluble guanylyl cyclase (sGC) by guanosine triphosphate (GTP), was introduced to assess CO vasodilatation at the cellular level.[2] Upon angiotensin II treatment, VSMCs exhibited a significant ratio increment which can be efficiently inhibited by NAC, revealing a $H_2O_2$ up-regulation during drug exposure (Figure S19). Meanwhile, a sharp up-regulation of cGMP level was observed in both angiotensin II and FB administrated VSMCs during light irradiation, demonstrating efficient CO releasing and its vasodilatation effect (Figure S20). Moreover, it can be found that, in the absence of angiotensin II, VSMCs treated with **FB** only showed no significant cGMP level change during irradiation, indicating the necessity of oxidative stress for realizing CO biological effect of **FB**. Subsequently, the vasodilatation effect of CO and angiotensin-II-induced $H_2O_2$ fluctuation *in vivo* were

mapped in transgenic line of zebrafish, Tg (flila: EGFP), which vascular endothelium was highlighted with green fluorescent protein (GFP) (Figure S21). Upon drug administration, the GFP-labelled zebrafish showed apparent vasoconstriction with vascular diameter sharply decreasing from 24.5 μm to 16.7 μm, indicating the vasoconstriction effect of angiotensin II (Figure 5). Correspondingly, compared with angiotensin-II-free treatment group (Figure 5a), the obvious fluorescent ratio increment of **FB** in zebrafish was observed, thus hinting $H_2O_2$ upregulation during angiotensin II administration. To consolidate this conclusion, the zebrafish was exposed to NAC after angiotensin II administration (Figure S22). It was shown that the increased ratio value was effectively attenuated by NAC. Therefore, it was credible to draw the conclusion that the $H_2O_2$ level was indeed upregulated during angiotensin II treatment. Then, the vasodilating capability of CO was explored. The zebrafish loaded with angiotensin II and **FB** was irradiated with TP laser to release CO (Figure 5c). The morphological observation of blood vessel displayed significant vasodilatation with the vascular diameter recovering from 16.7 μm to 23.8 μm (Figure 5g), thus apparently exhibiting the potent hemangiectasis effect of CO. In sharp contrast, in the absence of **FB**, the vessel of zebrafish with angiotensin II administration exhibited negligible morphological change during irradiation (Figure S23). In addition, upon NAC treatment after angiotensin II exposure, no vascular diameter change was observed during irradiation, implying no vasodilatation occurred without oxidative stress activation of **FB** (Figure S22). Taken these results together, the evidence of oxidative stress associated with $H_2O_2$ upon angiotensin II administration was provided, and the direct visualization of vasodilation effect of CO was realized.

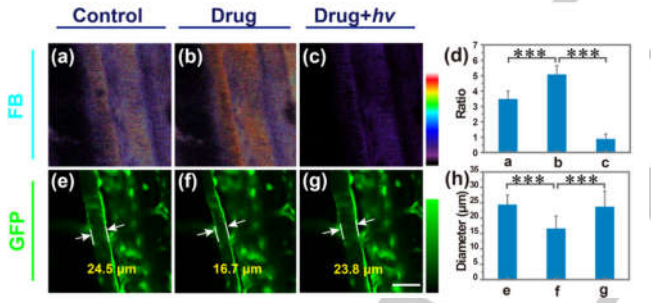


**Figure 5.** The vasodilatation effect of CO and angiotensin-II-induced $H_2O_2$ fluctuation. (a) and (e) Tg zebrafish was soaked with 20 μM **FB** (15 min). (b) and (f) Tg zebrafish was exposed to angiotensin II (2 h) after soaked with **FB** (15 min). (c) and (g) Tg zebrafish was irradiated with 800 nm laser for 5 min after treated with **FB** and angiotensin II. (d) The ratio changes of (a-c), (h) The blood vessel diameter changes of (e-g). The values are the mean ± s.d. for n = 3, ***p <0.001. Scale bar = 50 μm.

In conclusion, we have presented a new dual functional platform, **FB**, for $H_2O_2$ sensing and CO releasing. With two-photon excitation and ratiometric feedbacks, the two-stage behaviors of **FB** for $H_2O_2$ detection and photo-driven CO releasing were successfully implemented and monitored *in vitro* and *in vivo*. By capitalizing on the outstanding features of **FB**, oxidative stress in association with $H_2O_2$ was revealed upon angiotensin II administration, and the potent vasodilation effect of CO was mapped straightforwardly. Therefore, we anticipate that the superior features of **FB** will endow it with potential application for oxidative stress warning and CO photo-controlled release.

## Acknowledgements

This work was supported by the National Natural Science Foundation of China (21390411, 21535004, 91753111, 21775093, and 21505088).

**Keywords:** carbon monoxide photo-releasing • oxidative stress • two-photon control • vasodilatation • fluorescent imaging

[1] a) R. Motterlini, L. E. Otterbein, *Nat. Rev. Drug Discov.* **2010**, *9*, 728-743; b) S. W. Ryter, J. Alam, A. M. Choi. *Physiol. Rev.* **2006**, *86*, 583-650.

[2] K. Ling, F. Men, W. C. Wang, Y. Q. Zhou, H. W. Zhang, D. W. Ye, *J. Med. Chem.* **2017**. DOI: 10.1021/acs.jmedchem.6b01153.

[3] a) I. Chakraborty, S. J. Carrington, P. K. Mascharak, *Acc. Chem. Res.* **2014**, *47*, 2603-2611; b) N. Abeyrathna, K. Washington, C. Bashur, Y. Liao, *Org. Biomol. Chem.* **2017**, *15*, 8692-8699.

[4] a) L. K. C. De La Cruz, S. L. Benoit, Z. Pan, B. Yu, R. J. Maier, X. Ji, B. Wang, *Org. Lett.* **2018**. DOI: 10.1021/acs.orglett.7b03348; b) D. Wang, E. Viennois, K. Ji, K. Damera, A. Draganov, Y. Zheng, C. Dai, D. Merlin, B. Wang, *Chem. Commun.* **2014**, *50*, 15890-15893.

[5] a) P. Peng, C. Wang, Z. Shi, V. K. Johns, L. Ma, J. Oyer, A. Copik, R. Igarashi, Y. Liao, *Org. Biomol. Chem.* **2013**, *11*, 6671-6674; b) L. A. Antony, T. Slanina, Š. P, Š. T, P. Klán, *Org. Lett.* **2013**, *15*, 4552-4555; c) S. N. Anderson, J. M. Richards, H. J. Esquer, A. D. Benninghoff, A. M. Arif, L. M. Berreau, *ChemistryOpen* **2015**, *4*, 590-594; d) T. Soboleva, H. J. Esquer, A. D. Benninghoff, L. M. Berreau, *J. Am. Chem. Soc.* **2017**, *139*, 9435-9438.

[6] a) X. Jiao, Y. Li, J. Niu, X. Xie, X. Wang, B. Tang, *Anal. Chem.* **2018**, *90*, 533-555; b) P. Li, L. Liu, H. Xiao, W. Zhang, L. Wang, B. Tang, *J. Am. Chem. Soc.* **2016**, *138*, 2893-2896; c) Y. Li, X. Xie, X. Yang, M. Li, X. Jiao, Y. Sun, X. Wang, B. Tang, *Chem. Sci.* **2017**, *8*, 4006-4011.

[7] Y. Li, X. Wang, J. Yang, X. Xie, M. Li, J. Niu, L. Tong, B. Tang, *Anal. Chem.* **2016**, *88*, 11154-11159.

[8] a) C. R. Reczek, N. S. Chandel, *Curr. Opin. Cell Biol.* **2015**, *33*, 8-13; b) H. Sies, C. Berndt, D. P. Jones, *Annu. Rev. Biochem.* **2017**, *86*, 715-748.

[9] a) H. W. Liu, K. Li, X. X. Hu, L. Zhu, Q. Rong, Y. Liu, X. B. Zhang, J. Hasserodt, F. L. Qu, W. Tan, *Angew. Chem. Int. Ed.* **2017**, *56*, 11788-11792; b) X. Xie, J. Fan, M. Liang, Y. Li, X. Jiao, X. Wang, B. Tang, *Chem. Commun.* **2017**, *53*, 11941-11944.

[10] B. Liu, J. Wang, G. Zhang, R. Bai, Y. Pang, *ACS Appl. Mater. Interfaces* **2014**, *6*, 4402-4407.

[11] N. Inoue, S. Kinugawa, T. Suga, T. Yokota, K. Hirabayashi, S. Kuroda, K. Okita, H. Tsutsui, *Am. J. Physiol. Heart Circ. Physiol.* **2012**, *302*, H1202-1210.

[12] a) Y. Xu, X. Sui, J. Jiang, J. Zhai, L. Gao, *Adv. Mater.* **2016**, *28*, 10780-10785; b) M. Di Pascoli, D. Sacerdoti, P. Pontisso, P. Angeli, M. Bolognesi, *J. Vasc. Res.* **2017**, *54*, 92-99.

10.1002/anie.201805806




**Entry for the Table of Contents** (Please choose one layout)

Layout 1:

## COMMUNICATION

We engineered a two-photon fluorescent molecule featuring capacity of highly sensitive and specific $H_2O_2$ sensing and photo-induced CO releasing.

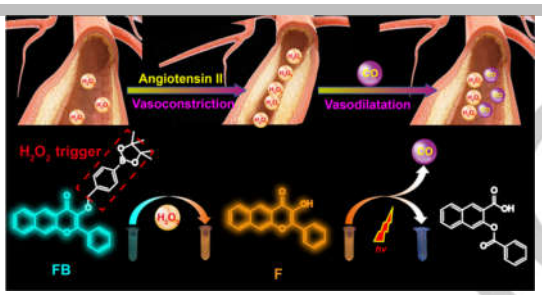


*Yong Li, Yingzheng Shu, Muwen Liang, Xilei Xie, Xiaoyun Jiao, Xu Wang* and Bo Tang**

***Page No. – Page No.***
**A Two-photon $H_2O_2$-activated CO Photoreleaser**